# Structure and Cohesive Properties of Sphingomyelin/Cholesterol Bilayers†

Thomas J. McIntosh,*,‡ Sidney A. Simon,§ David Needham,‖ and Ching-hsien Huang⊥

*Departments of Cell Biology, Neurobiology, and Anesthesiology, Duke University Medical Center, Durham, North Carolina 27710, Department of Mechanical Engineering and Materials Science, Duke University, Durham, North Carolina 27706, and Department of Biochemistry, University of Virginia School of Medicine, Charlottesville, Virginia 22908*

*Received September 10, 1991; Revised Manuscript Received November 21, 1991*

ABSTRACT: Thermal, structural, and cohesive measurements have been obtained for both bovine brain sphingomyelin (BSM) and *N*-tetracosanoylsphingomyelin (C24-SM) in the presence and absence of cholesterol. A goal of these experiments has been to clarify the mechanisms responsible for the strong interaction between sphingomyelin and cholesterol. Differential scanning calorimetry shows that fully hydrated bilayers of BSM and C24-SM have main endothermic phase transitions at 39 and 46 °C, respectively, that reflect the melting of the acyl chains from a gel to a liquid-crystalline phase. For each lipid, the addition of cholesterol monotonically reduces the enthalpy of this transition, so that at equimolar cholesterol the transition enthalpy is zero. The addition of equimolar cholesterol to either BSM or C24-SM coverts the wide-angle X-ray diffraction reflection at 4.15 Å to a broad band centered at 4.5 Å. Electron density profiles of gel-phase C24-SM bilayers contain two terminal methyl dips in the center of the bilayer, indicating that the lipid hydrocarbon chains partially interdigitate so that the long saturated 24-carbon acyl chains in one monolayer cross the bilayer center and appose the shorter sphingosine chains from the other monolayer. The incorporation of cholesterol adds electron density to the hydrocarbon chain region near the head group and removes the double terminal methyl dip. These wide- and low-angle X-ray data indicate that cholesterol packs into the hydrocarbon chain region near the sphingomyelin head group, fluidizes the methylene chains near the center of the bilayer compared to the gel phase, and reduces the extent of methylene chain interdigitation. This reduction of chain interdigitation by cholesterol could reduce the possibility of energetically unfavorable voids in the center of biological membranes that contain sphingomyelin. Isothermal compressibility moduli are similar for bilayers composed of equimolar cholesterol and either BSM, C24-SM, or saturated long-chain phosphatidylcholines but are significantly higher than published values for equimolar cholesterol with unsaturated phosphatidylcholines. These compressibility data suggest that the strong interaction between sphingomyelin and cholesterol arises from the van der Waals interactions between cholesterol and saturated lipid acyl chains and that there is no specific hydrogen-bond formation between cholesterol and sphingomyelin. Although the acyl chain of BSM may contain a double bond, we argue that BSM interacts strongly with cholesterol because the principle unsaturated fatty acid of BSM (nervonic acid) has its cis double bond at the 15 position, which is far enough down the chain to not affect the cholesterol–acyl chain interaction.

Sphingomyelin (SM) is a polar lipid which is a major component of the plasma membranes of many animal cells. Sphingomyelin and the common membrane lipid phosphatidylcholine (PC) both contain the same phosphorylcholine polar head group (Figure 1). However, sphingomyelins differ in several significant ways from most naturally occurring phosphatidylcholines. First, the backbone of SM is sphingosine, whereas the backbone of PC is glycerol. Second, the hydrophobic region of SM consists of the relatively short paraffinic residue of sphingosine and an acyl chain that is usually quite long and most often is fully saturated or contains a single cis double bond. Typically the acyl chain of naturally occurring SM is longer than 20 carbons, and the average number of cis double bonds per SM molecule is 0.1–0.35, compared to 1.1–1.5 per typical membrane PC molecule (Barenholz & Thompson, 1980). This means that the hydrophobic region of the SM molecule, in contrast to most PCs, is relatively saturated and is quite asymmetric, with the acyl chain being much longer than the sphingosine chain.

Biological membranes that contain appreciable amounts of sphingomyelin invariably contain high concentrations of cholesterol. Numerous studies have shown that there is a strong interaction between sphingomyelin and cholesterol. For example, cholesterol condenses sphingomyelin monolayers more than it condenses monolayers of other phospholipids (Lund-Katz et al., 1988), the water permeability is lower for sphingomyelin/cholesterol bilayers than for other lipid bilayers (Barenholz, 1986; Finkelstein, 1987), the rate of cholesterol desorption is much smaller from SM bilayers than from other types of phospholipid bilayers (Lund-Katz et al., 1988), and the compressibility modulus of equimolar bovine brain sphingomyelin/cholesterol bilayers is over two times larger than that of equimolar stearoyloleoylphosphatidylcholine/cholesterol bilayers (Needham & Nunn, 1990).

The physical–chemical properties of sphingomyelin/cholesterol bilayers have been studied by a variety of techniques, including X-ray diffraction (Khare & Worthington, 1977), differential scanning calorimetry (Calhoun & Shipley, 1979a; Estep et al., 1979), nuclear magnetic resonance (Oldfield & Chapman, 1972; Cullis & Hope, 1980), and micropipet aspiration (Needham & Nunn, 1990). It has been a long-standing question whether the strong interaction between

† This research was supported by grants from the National Institutes of Health (GM-27278 and GM-40162).

* To whom correspondence should be addressed.

‡ Department of Cell Biology, Duke University Medical Center.

§ Departments of Neurobiology and Anesthesiology, Duke University Medical Center.

‖ Department of Mechanical Engineering and Materials Science, Duke University.

⊥ Department of Biochemistry, University of Virginia School of Medicine.

0006-2960/92/0431-2012$03.00/0 

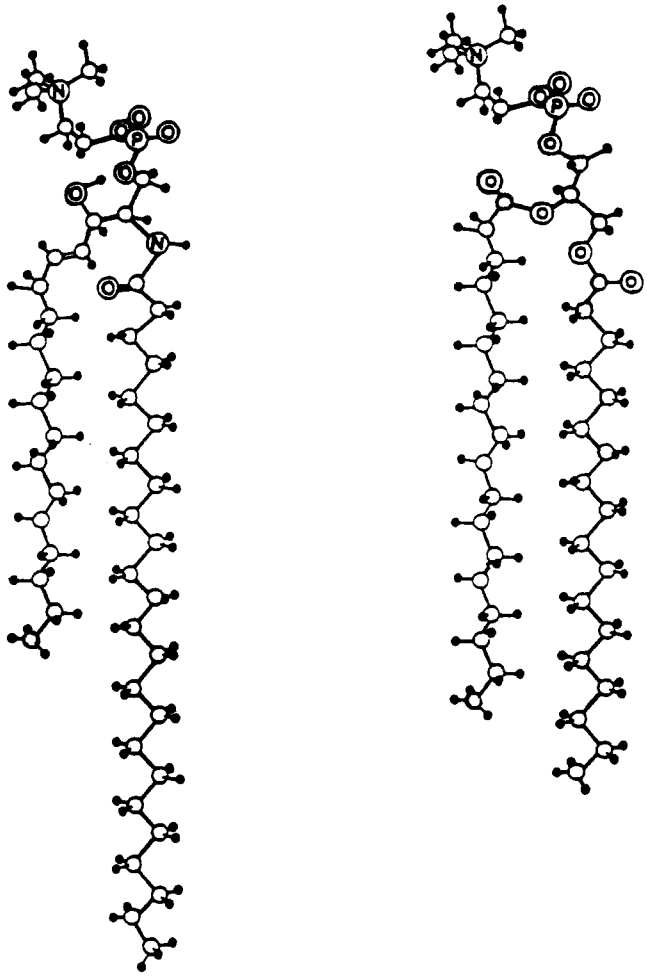

FIGURE 1: Structural models of C24-SM (left) and phosphatidylcholine (right).

cholesterol and sphingomyelin is mediated by hydrogen bonding between cholesterol and the sphingosine backbone (Barenholz et al., 1980; Boggs, 1987) or by van der Waals interactions between cholesterol and the SM hydrocarbon chains (Vanderheuvel, 1963; Lund-Katz et al., 1988; Kan et al., 1991).

In this paper, we determine the effects of cholesterol on the thermal, structural, and cohesive properties of two sphingomyelins, naturally occurring bovine brain sphingomyelin (BSM) and a synthetic sphingomyelin whose acyl chain is saturated and contains 24 carbons (C24-SM). The goal of these experiments is to provide information concerning the mechanism of the strong sphingomyelin–cholesterol interaction. In particular, we want to determine which structural feature of the sphingomyelin molecule gives rise to the strong interaction with cholesterol: the sphingosine backbone, the unusually long saturated acyl chain, or the the asymmetric hydrocarbon chain region. In the following paper in this issue (McIntosh et al., 1992), we analyze the interbilayer interactions for SM and SM/cholesterol systems.

## Materials and Methods

*Materials.* BSM, egg SM, and dipalmitoylphosphatidylcholine [C(16:0)C(16:0)PC] were obtained from Avanti Polar Lipids, Inc. (Birmingham, AL). The acyl chain composition of BSM (as supplied by Dr. Walter Shaw of Avanti Polar Lipids) was 42.4% 18:0, 5.9% 20:0, 10.3% 22:0, 8.9% 24:0, and 17.0% 24:1, with other components less than 5%. This chain length distribution is consistent with that found by Calhoun and Shipley (1979a). *N,N*-Dicyclohexylcarbodimide, cholesterol, and poly(vinylpyrrolidone) (PVP) with an average molecular weight of 40 000 were purchased from Sigma Chemical Co. (St. Louis, MO). Tetracocasonoic acid was obtained from Aldrich Chemical Co. (Milwaukee, WI).

*Semisynthesis of C(12:0)C(22:0)PC and C(22:0)C(12:0)PC.* Mixed-chain phosphatidylcholines, C(12:0)C(22:0)PC and C(22:0)C(12:0)PC, were synthesized by a reacylation of an appropriate 1-acyllysophosphatidylcholine with a fatty acid anhydrite at room temperature as described previously (Xu & Huang, 1987; Lin et al., 1990).

*Semisynthesis of N-Tetracosanoyl Sphingomyelin (C24-SM).* The semisynthesis involves two major steps: the deacylation of egg sphingomyelin and the reacylation of sphingosylphosphocholine with tetracosanoic acid (Gaver & Sweeley, 1965; Cohen et al., 1984; Scripada et al., 1987). Briefly, egg sphingomyelin (1.5 mM) was dispersed in 150 mL of 1 N methanolic HCl. The mixture was heated at 70 °C for 30 h, and then the solvent was removed by rotary evaporation. The precipitate was suspended in 2-propanol and evaporated by rotatory evaporating three times followed by silicic acid column chromatography ($CHCl_3$/MeOH/$H_2O$). The product, sphingosylphosphocholine hydrochloric acid salt, appeared as a single spot, $R_f$ = 0.07, on a thin-layer plate developed in $CHCl_3$/MeOH/25% $NH_4OH$/$H_2O$ (55:35:1:4). After being dispersed in dry chloroform and neutralized with triethylamine, sphingosylphosphocholine was reacylated with tetracosanoic acid (4.1 mM) in the presence of dicyclohexylcarbodimide (13.9 mM) at room temperature for 1 h. The reaction was then allowed to proceed at 35 °C for 2 h. After filtering, the residue was subjected to silicic acid column chromatography. The product, *N*-tetracosanoylsphingomyelin (C24-SM) was eluted off the column with a gradient of $CHCH_3$/MeOH; it showed a single $R_f$ value of 0.17 on TLC plate developed with a mixture of $CHCl_3$/MeOH/25% $NH_4$/$H_2O$ (55:35:1:4).

*Differential Scanning Calorimetry.* For C24-SM, differential scanning calorimetry measurements were made with a high-resolution MC-2 differential scanning calorimeter with cooling capability (Microcal Inc., Northampton, MA) that was interfaced to an IBM-PC computer. The differential voltage signal from the thermopiles and the temperature of the heat sink were recorded every 10 s on the computer. Each sample was scanned at least three times at a constant scan rate of 15 °C/h in the following sequence: initial heating, cooling, and second heating. The transition temperatures and calorimetric enthalpies were evaluated by the software package provided by Microcal Inc., as described elsewhere (Xu & Huang, 1987).

Bovine brain sphingomyelin/cholesterol dispersions in excess water were formed as follows. BSM and cholesterol were first codissolved in chloroform. The chloroform was removed under vacuum, and the dried lipid was transferred into a calorimetry sample pan. Excess water was then added, and the sample pan was hermetically sealed and heated to 60 °C for 30 min. Differential scanning calorimetry measurements were performed using a Perkin-Elmer DSC7 calorimeter with the Perkin-Elmer Corp. data station. The samples were scanned at rates of 5 °C/min in both heating and cooling cycles. Transition enthalpies were calculated by integrating the area under the heat capacity–temperature curve.

*X-ray Diffraction.* For C24-SM and BSM, in the presence and absence of cholesterol, X-ray diffraction patterns were recorded from both unoriented dispersions and oriented multilayers. For the unoriented multiwalled liposomes, water content was varied by the "osmotic stress" method (LeNeveu

et al., 1977; Parsegian et al., 1979, 1986). In brief, an excess amount of the appropriate PVP solution was added to the dry lipid. The suspensions were covered with nitrogen and incubated for several hours with periodic vortexing above the lipid's main phase transition temperature. Because PVP molecules are too large to enter between the lipid multilayers, they compete for water and thereby compress the lipid lattice (LeNeveu et al., 1977; Parsegian et al., 1986). Osmotic pressures for the PVP/water solutions were previously measured (McIntosh et al., 1989c) and ranged from $1.1 \times 10^5$ to $3.2 \times 10^7$ dyn/cm$^2$. The lipid/polymer suspensions were sealed in quartz glass capillary tubes and mounted in a point-collimation X-ray diffraction camera.

Oriented multilamellar specimens were formed by placing a small drop of lipid/chloroform solution on a piece of aluminum foil and slowly evaporating the chloroform. The foil substrate was given a convex curvature and mounted in a controlled humidity chamber on a line-focused single-mirror X-ray camera, where the X-ray beam was oriented at a grazing angle relative to the lipid multilayers. The humidity chamber consisted of a canister with two mylar windows for passage of the X-ray beam. Pressures in the range of $2.8 \times 10^7$ to $2.3 \times 10^9$ dyn/cm$^2$ were applied through the vapor phase to oriented lipid multilayers by the use of established procedures (Parsegian et al., 1979; McIntosh et al., 1987). The vapor pressure was controlled by means of a cup of saturated salt solution in the chamber. To speed equilibration, a gentle stream of nitrogen gas was passed through a flask of the saturated salt solution and through the chamber. For the salt solutions used in these experiments, the ratio of the vapor pressure ($p$) of the saturated salt solution to the vapor pressure of pure water ($p_0$) has been measured (O'Brien, 1948; Weast, 1984). The following saturated salt solutions were used to obtain the relative vapor pressures ($p/p_0$) indicated in parentheses: $CuSO_4$ (0.98), $Na_2SO_4$ (0.93), KCl (0.87), $NH_4Cl$ (0.80), $NaNO_2$ (0.66), $CaCl_2$ (0.32), and $KC_2H_3O_2$ (0.20). The applied pressure is given by $P = -(RT/V_w) \ln (p/p_0)$ where $R$ is the molar gas constant, $T$ is the temperature (293 ± 2 K for the experiments reported here), and $V_w$ is the molar volume of water.

For all specimens, oriented multilayers and unoriented lipid/polymer suspensions, X-ray diffraction patterns were recorded at 20 °C on Kodak DEF X-ray film. X-ray films were processed by standard techniques and densitometered with a Joyce-Loebl microdensitometer as described previously (McIntosh & Simon, 1986a,b; McIntosh et al., 1987). After background subtraction, integrated intensities, $I(h)$, were obtained for each order $h$ by measuring the area under each diffraction peak. For unoriented patterns, the structure amplitude $F(h)$ was set equal to $[h^2I(h)]^{1/2}$ (Blaurock & Worthington, 1966; Herbette et al., 1977). For the oriented line-focused patterns, the intensities were corrected by a single factor of $h$ due to the cylindrical curvature of the multilayers (Blaurock & Worthington, 1966; Herbette et al., 1977) so that $F(h) = [hI(h)]^{1/2}$.

Electron density profiles, $\rho(x)$, on a relative electron density scale were calculated from

$$\rho(x) = (2/d)\sum \exp[\phi(h)]F(h) \cos (2\pi xh/d) \quad (1)$$

where $x$ is the distance from the center of the bilayer, $d$ is the lamellar repeat period, $\phi(h)$ is the phase angle for order $h$, and the sum is over $h$. Phase angles were determined by the use of the sampling theorem (Shannon, 1949) as described in detail previously (McIntosh & Holloway, 1987). All electron density profiles described in this paper are at a resolution of $d/2h_{max} \approx 6$ Å.

*Measurements of Cohesive Properties by Micromanipulation.* The preparation of giant unilamellar vesicles from lipid solutions and the procedures for carrying out thermomechanical studies have been well documented in several recent publications concerning the micromanipulation of such structures (Kwok & Evans, 1981; Needham & Evans, 1988; Needham & Hochmuth, 1989; Needham & Nunn, 1990). Briefly, lipid/cholesterol mixtures were dissolved in chloroform/methanol and dried onto a teflon substrate. Vesicles were formed by gently rehydration of the dried lipid lamellae using an aqueous solution containing 160 mOsm sucrose. Sucrose-containing vesicles were suspended in a hyperosmotic glucose solution in the micromanipulation chamber.

Although few in number, large unilamellar vesicles (20–40 μm in diameter) were identified and aspirated by micropipet such that a small projection was produced in the suction pipet. After a prestress, the pipet suction pressure was increased and then decreased in increments by means of a water-filled manometer and suction syringe, and the corresponding change in vesicle projection length in the pipet was recorded on video. Micropipet suction pressure was measured via an in-line pressure transducer. Subsequent analysis of pipet and vesicle geometry allowed the calculation of the membrane area change in response to the induced membrane tension due to pressurization (Kwok et al., 1981).

The experiments were caried out in a temperature-controlled chamber at 15 °C. At this temperature, changes in osmolarity due to evaporation losses, and concomitant decreases in vesicle volume, were negligible during the time course of the measurement. Also, the presence of trapped solutes in the vesicles minimized volume changes due to water filtration. Thus, the changes in projection length in the pipet as a result of changes in isotropic membrane tension were solely due to membrane area changes and not volume changes. The elastic area compressibility modulus was determined from the slope of plots of membrane isotropic tension vs relative area change (Kwok & Evans, 1981). The pipet and the microchamber were electrically grounded, which, together with a precoating of the pipet and glass chamber surfaces with albumin, greatly reduced the incidence of premature vesicle lysis.

## Results

*Differential Scanning Calorimetry.* After incubation of the C24-SM dispersion at 0 °C for 6 days, the initial heating curve contained two endothermic transitions, with peaks at 39.5 °C (enthalpy, $\Delta H$ = 4.1 kcal/mol) and 46.2 °C ($\Delta H$ = 6.3 kcal/mol) (data not shown). The high-temperature transition remained unchanged in peak temperature and enthalpy upon subsequent cooling or immediate reheating, whereas the low-temperature transition changed its position and area in the first cooling scan ($T_m$ = 39.8 °C and $\Delta H$ = 2.5 kcal/mol) and also in the second heating scan ($T_m$ = 39.6 °C and $\Delta H$ = 2.8 kcal/mol). The second heating scan for a dispersion of C24-SM is shown in Figure 2A. The transition peaks of C24-SM were abolished completely upon incorporation of 50 mol % cholesterol (data not shown).

Thermograms of hydrated BSM bilayers which had previously been annealed in the liquid-crystalline phase exhibited a maximum heat capacity at 39.2 °C with lower and higher temperature shoulders extending to about 35 and 42 °C, respectively (Figure 2B). These values are consistent with those of Calhoun and Shipley (1979a). The maximum transition at 39.2 °C likely represents the melting of the fraction (42%) of BSM containing a stearoyl fatty acid chain (C18:0), and the shoulders at higher and lower temperatures represent the melting of BSM with longer and shorter fatty acid chains,

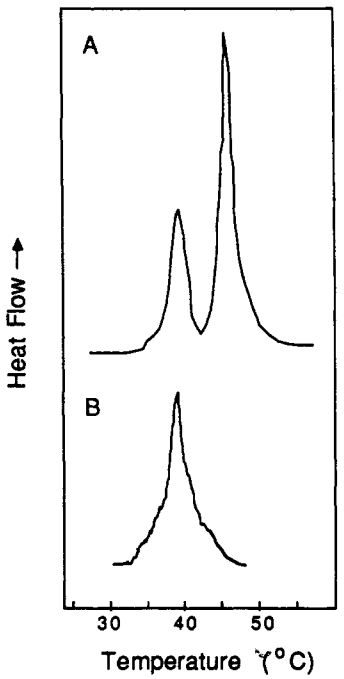


FIGURE 2: Differential scanning calorimetry thermograms for (A) fully hydrated C24-SM bilayers and (B) fully hydrated bovine sphingomyelin bilayers. Thermogram A is the second heating run after a 6-day incubation at 0 °C. Thermogram B is the first heating run after incubation at 60 °C and cooling to 20 °C. The heat flow axis is in arbitrary units and the transition enthalpies are given in the text.

respectively (Marsh, 1990). The total enthalpy of this transition was $\Delta H = 5.84 \pm 0.27$ kcal/mol ($N = 4$). The endothermic peak did not markedly shift with the incorporation of cholesterol up to equimolar concentrations, although the transition width greatly broadened (not shown). The transition enthalpy decreased with increasing cholesterol content, until no transition was observable at 50 mol % cholesterol (Figure 3), in agreement with the results of Oldfield and Chapman (1972).

*X-ray Diffraction.* For all oriented and unoriented SM and SM/cholesterol speimens at 20 °C, the X-ray diffraction patterns consisted of a series of low-angle reflections, which indexed as orders of a lamellar repeat period, and a single wide-angle band. Wide-angle patterns from bilayers of BSM or C24-SM contained reflections centered at 4.15 Å, a spacing typical for phospholipids in the gel phase (Tardieu et al., 1973). This wide-angle reflection extended from 4.12 to 4.17 Å and was broader than the extremely sharp reflections which were observed previously with the same X-ray camera for gel phase bilayers with untilted hydrocarbon chains (McIntosh, 1980; McIntosh et al., 1989b). The breadth of this reflection indicates that the hydrocarbon chains are tilted at an angle relative to the plane of the bilayer (Tardieu et al., 1973; McIntosh, 1980; McIntosh et al., 1989b). For all equimolar BSM or C24-SM/cholesterol bilayers, the wide-angle pattern consisted of a very broad wide-angle band centered at about 4.5 Å. This type of broad wide-angle band is typical of liquid-crystalline ($L_\alpha$) phase bilayers (Tardieu et al., 1973). For each sample the wide-angle pattern was independent of applied osmotic pressure.

For C24-SM, the lamellar repeat period ranged from 74.3 Å for $P = 4.3 \times 10^5$ dyn/cm$^2$ (corresponding to 10% PVP) to 63.8 Å for $P = 2.3 \times 10^9$ dyn/cm$^2$ (corresponding to a relative vapor pressure of 0.20). Structure factors for these diffraction experiments are shown as solid circles in Figure

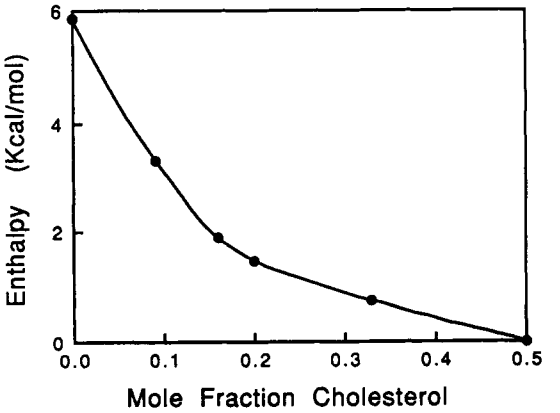


FIGURE 3: Plot of transition enthalpy ($\Delta H$) versus mole fraction cholesterol for fully hydrated BSM bilayers.

4A. The solid line is the continuous Fourier transform calculated using the sampling theorem (Shannon, 1949) and one particular data set. Since all of the structure factors fall close to this line, the structure of the bilayer is approximately constant at all applied pressures (Torbet & Wilkins, 1976; McIntosh et al., 1986b, 1989a). For BSM, equimolar C24-SM/cholesterol, and equimolar bovine brain SM/cholesterol, the ranges of measured repeat periods were 75.6–63.4, 68.1–66.3, and 66.3–59.3 Å, respectively. For all experiments, five or six lamellar diffraction orders were obtained, depending on the lamellar repeat period. Structure factors for bovine brain SM, equimolar C24-SM/cholesterol, and equimolar bovine brain SM/cholesterol are shown as solid circles in Figure 4, panels B, C, and D, respectively. Again, for each of these samples, the structure factors fall close to the continuous transform (solid lines), indicating the structure does not change with increasing osmotic pressure. For both C24-SM and bovine brain SM bilayers with cholesterol, the range of repeat periods obtained, and therefore the number of data points in reciprocal space (Figure 4C,D) are smaller than those obtained for C24-SM bilayers and BSM bilayers (Figure 4A,B). This is because phase separation occurred for specimens containing cholesterol for applied pressures greater than $2 \times 10^7$ dyn/cm$^2$, and structure factors from experiments with phase separation are not included in Figure 4C,D. That is, at these high pressures, additional X-ray reflections were recorded at 34 Å, indicative of a separate cholesterol phase (Khare et al., 1977; Khare & Worthington, 1978).

Figure 5 shows electron density profiles for C24-SM bilayers (top) and equimolar C24-SM/cholesterol bilayers (bottom), and Figure 6 shows electron density profiles for BSM bilayers (top) and equimolar BSM/cholesterol bilayers (bottom). For each profile, the high-density peaks, located at about ±25 Å from the bilayer center, correspond to the high-density lipid head groups, and the lower electron density region in the center of the profile corresponds to the lipid hydrocarbon chains. Both the distance between head group peaks across the bilayer and the shape of the low-density hydrocarbon interior of the bilayer are somewhat different for the four systems. The distances between the peaks in the electron density profiles for the range of applied pressures were found to be 51.0 ± 0.4 Å (mean ± standard deviation, $N = 7$ experiments), 50.1 ± 0.8 Å ($N = 21$), 50.9 ± 0.7 Å ($N = 4$), and 45.5 ± 0.6 Å ($N = 7$) for C24-SM, BSM, 1:1 C24-SM/cholesterol, and 1:1 BSM/cholesterol, respectively. For BSM bilayers, the electron density profile (Figure 6, top) contains a deep trough in the center of the bilayer, corresponding to a preferential localization of the low-density terminal methyl groups of the hydrocarbon chains in the geometric center of the bilayer. For

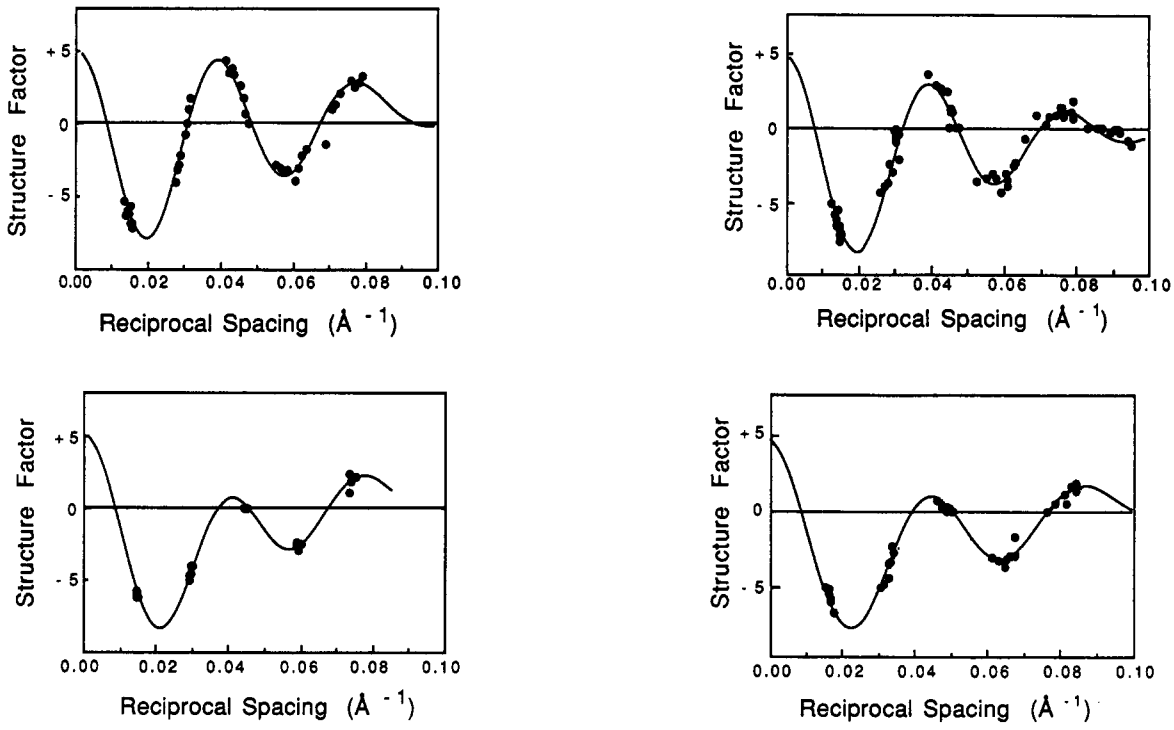


FIGURE 4: X-ray diffraction structure factors for bilayers of (A, top left) C24-SM, (B, top right) bovine brain SM, (C, bottom left) equimolar C24-SM/cholesterol, and (D, bottom right) equimolar bovine brain SM/cholesterol. The solid circles represent observed structure factors for osmotic stress experiments, and the solid curves are reconstructions of the continuous transforms calculated using the sampling theorem.

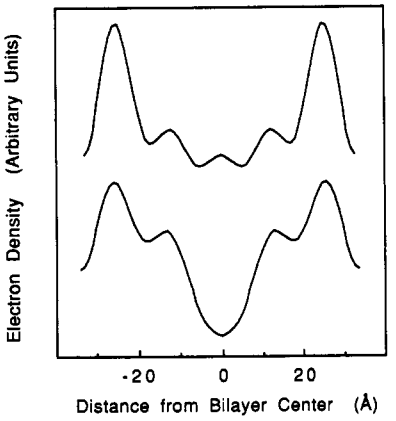


FIGURE 5: Electron density profiles for bilayers of C24-SM (top) and equimolar C24-SM/cholesterol (bottom).

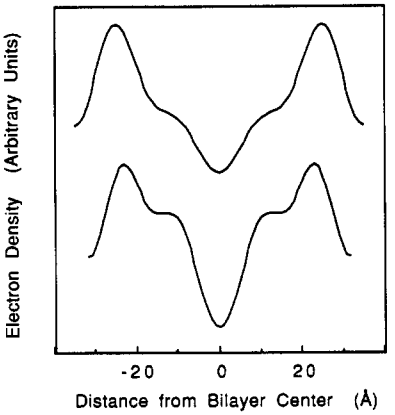


FIGURE 6: Electron density profiles for bilayers of BSM (top) and equimolar BSM/cholesterol (bottom).

C24-SM, the profile (Figure 5, top) contains a wider, low-density region, with low-density dips located about 5 Å from the geometric center of the bilayer. This shape for the low-density region indicates that for C24-SM bilayers the terminal methyl groups are not localized in the geometric center of the bilayer. For all profiles (Figure 5 and 6), the medium-density shoulders located between the head group peak and the terminal methyl trough correspond to methylene groups of the hydrocarbon chains. In the profiles of bilayers containing cholesterol (Figures 5 and 6, bottom), the methylene chain region shoulders are significantly higher in density than are the same regions in the corresponding profiles of bilayers without cholesterol (Figures 5 and 6, top). Previously, the addition of cholesterol has been shown to add density to the methylene chain region of phosphatidylcholine bilayers (Franks, 1976; McIntosh, 1978; McIntosh et al., 1989a).

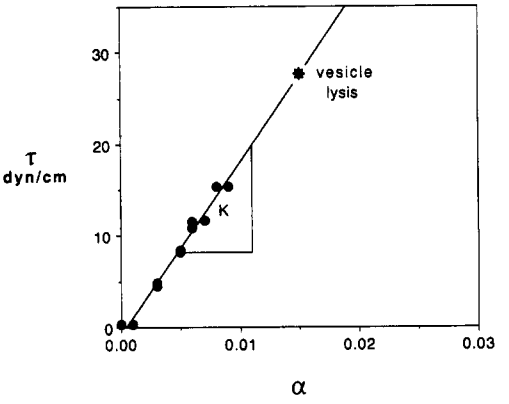


FIGURE 7: Plot of isotropic tension ($\tau$) versus area dilation ($\alpha$) for equimolar C24-SM/cholesterol bilayers. The slope of the straight line is the compressibility modulus (K).

*Cohesive Properties.* A graph of the isotropic tension ($T$) versus the area dilation ($\alpha$) for equimolar C24-SM/cholesterol bilayers at 15 °C is shown in Figure 7. The slope of this line yields the compressibility modulus ($K$), which is 1799 ± 234 dyn/cm for C24-SM/cholesterol bilayers. For comparison, Table I shows previously published values of $K$ for equimolar BSM/cholesterol, C(18:0)C(18:1)PC/cholesterol, and C-

Table I: Cohesive Properties[a]

| lipid | mol % cholesterol | $K$ (dyn/cm) |
|---|---|---|
| C24-SM | 50 | 1799 ± 234 |
| BSM | 50 | 1718 ± 484 |
| C(16:0)C(16:0)PC | 50 | 2235 ± 396 |
| C(22:0)C(12:0)PC | 50 | 1721 ± 220 |
| C(12:0)C(22:0)PC | 50 | 1889 ± 217 |
| C(18:0)(18:1)PC | 0 | 193 ± 20 |
| C(18:0)(18:1)PC | 50 | 710 ± 48 |
| C(20:4)(20:4)PC | 0 | 57 ± 14 |
| C(20:4)(20:4)PC | 50 | 102 ± 24 |

[a] Data for C(18:0)(18:1)PC, C(20:4)(20:4)PC, and BSM are taken from Needham and Nunn (1990).

(20:4)C(20:4)PC/cholesterol bilayers. The values of $K$ for equimolar C24-SM/cholesterol are similar to those for equimolar BSM/cholesterol bilayers but are larger than those of C(18:0)C(18:1)PC/cholesterol and much larger than those of C(20:4)C(20:4)PC/cholesterol bilayers.

To determine whether the large values of $K$ for C24-SM/cholesterol and BSM/cholesterol bilayers are due to the sphingosine backbone, or to the length, saturation, or asymmetry of the hydrocarbon chains, we measured $K$ for equimolar mixtures of cholesterol with phospholipids with saturated symmetric acyl chains, (C16:0)C(16:0)PC, and saturated asymmetric acyl chains, C(12:0)C(22:0)PC and C(22:0)C-(12:0)PC. As shown in Table I, bilayers of equimolar cholesterol with BSM, C24-SM, C(12:0)C(22:0)PC, C(22:0)C-(12:0)PC, and C(16:0)(16:0)PC all have relatively large compressibility moduli.

## Discussion

*Thermal Properties.* Both BSM and C24-SM melt at temperatures above mammalian physiological temperature of 37 °C (Figure 2). Equimolar concentrations of cholesterol convert their gel phases into liquid-crystalline phases. This gel to liquid-crystalline conversion upon the addition of cholesterol is evidenced by the continuous reduction in the transition enthalpy (Figure 3) and the change in the wide-angle diffraction data, as well as by NMR data (Oldfield & Chapman, 1971).

For BSM bilayers, the single endothermic transition reflects the melting from a gel phase bilayer to a liquid-crystalline ($L_\alpha$) bilayer (Shipley et al., 1974). The fact that this transition is relatively broad compared to the transition for C24-SM (Figure 2A,B) reflects the large chain length heterogeneity found in BSM (Barenholz, 1986). For C24-SM, there are two endothermic transitions. The higher temperature transition at 46 °C undoubtedly reflects the melting from a gel phase to the liquid-crystalline ($L_\alpha$) phase (Calhoun & Shipley, 1979b; Levin et al., 1985). The lower temperature transition probably represents a transition between two gel phases, since the enthalpy and temperature of the lower temperature transition depend on the amount of time of low-temperature incubation, as do the enthalpy and temperature of gel–gel phase transitions in saturated phosphatidylcholines (Lin et al., 1990). Although we did not attempt to determine the structure of the C24-SM phase which is present at temperatures between the two endotherms, it may be a rippled lamellar ($P_{\beta'}$) gel phase (Tardieu et al., 1973; Janiak et al., 1976, 1979), since the rippled phase is present in phosphatidylcholines which have tilted hydrocarbon chains and our X-ray data indicate that C24-SM also has tilted hydrocarbon chains (see below). That is, we argue that the endothermic transition at 39 °C corresponds to the "pretransition" endotherm observed for saturated phosphatidylcholines (Janiak et al., 1976, 1979). We note that the total enthalpy of the two transitions at 39 and 46 °C (about 9.1 kcal/mol) is similar to the total enthalpy of the pretransition and main transition found for C(18:0)C(18:0)PC (Marsh, 1990), a lipid with the same number of methylene groups in the hydrocarbon region. However, the ratio of enthalpies of the two peaks is different for the two lipids, as the enthalpy of the main transition for C(18:0)C(18:0)PC is higher than the enthalpy of the 46 °C transition of C24-SM and the enthalpy of the pre-transition for C(18:0)C(18:0)PC is lower than the enthalpy of 39 °C transition of C24-SM. This implies that the intermediate phase (possibly a rippled phase) contains more gauche conformers in C24-SM than in C(18:0)C(18:0)PC. In this regard, we note that pretransition endotherms with relatively large enthalpies have been observed for the mixed-chain PCs C(18:0)C(14:0)PC (Mason et al., 1981) and C(20:0)C-(14:0)PC (Lin et al., 1990).

*Structure.* The wide- and low-angle X-ray data provide detailed structural information on sphingomyelin bilayers in the presence and absence of cholesterol. First, consider the case of C24-SM bilayers. The wide-angle pattern indicates that the hydrocarbon chains are in the gel phase and are tilted relative to the bilayer normal. The electron density profile (Figure 5, top) shows an unusual shape for the central region of the bilayer. For gel phases from diacyl lipids with chains of equal length, such as C(16:0)(16:0)PC, electron density profiles have a single deep and sharp density dip in the center of the profile due to the localization of the lipid terminal methyl groups in the bilayer center (Lesslauer et al., 1972; Torbet & Wilkins, 1976; McIntosh, 1978, 1980). The broad trough, with dips located about 5 Å from the center of the profile, indicates that for C24-SM the methyl groups are not localized in the center of the bilayer. The wide-angle diffraction pattern, the shape of the central region of the profile, and the 51-Å distance between head-group peaks across the bilayer place severe constraints on the possible modes of hydrocarbon chain packing in the C24-SM bilayer. The following packing model fits all of the X-ray data. In this model, which is similar to packing models previously presented for a gel phase of mixed-chain phosphatidylcholine bilayers (Mason et al., 1981; Serrallach et al., 1984; Huang & Mason, 1986; Mattai et al., 1987) and DL-*erythro*-*N*-lignocerosylsphingosylphosphocholine (Levin et al., 1985) and the liquid-crystalline phase of C24-SM (Maulik et al., 1986), the long C24 chain crosses the center of the bilayer and apposes the short sphingosine chain. This packing arrangement would place the low-density terminal methyl groups of both the C24 and the sphingosine chain away from the geometric center of the bilayer and would be consistent with the electron density profile (Figure 5). If the chains were packed in this manner and were oriented perpendicular to the plane of the bilayer, molecular models indicate that the distance between head-group peaks across the bilayer would be expected to be about 57 Å. Since the observed distance between head-group peaks in the electron density profiles is about 51 Å, this indicates that, if the hydrocarbon chains were fully extended, they would be tilted by about 27°. This is a chain tilt similar to that found for gel phases of saturated phosphatidycholines (Tardieu et al., 1973; McIntosh, 1980; Wiener et al., 1989). We note that this is a rough estimate for the chain tilt, and must be considered an upper estimate, since we have ignored the effects of possible rotational isomers or "kinks", which would also reduce bilayer thickness. The reason for chain tilt in C24-SM bilayers is probably the same as that proposed for gel phase PC bilayers, namely that the lipid head group has a larger excluded area in the plane of the bilayer than the lipid hy-

drocarbon chains, so that the chains tilt to maximize van der Waals interactions (McIntosh, 1980). It should also be noted that lipids that have tilted chains in their gel phases, such as the saturated phosphatidylcholines, exhibit pretransitions at temperatures below the main melting transition (Janiak et al., 1979), similar to the one in our thermogram of C24-SM (Figure 2A).

A similar packing arrangement probably also holds for BSM as previously found by Khare and Worthington (1978), although the heterogeneity of chain lengths makes it impossible to estimate the lipid chain tilt. We argue that the chain tilt is probably somewhat less for BSM compared to C24-SM, since the bilayer thickness is about the same for the two lipids, and the average acyl chain length is less for BSM. The heterogeneity in chain length for BSM would tend to spread the distribution of the terminal troughs across the center of the bilayer, accounting for the somewhat broader low density trough in the profile of BSM (Figure 6) than in profiles of gel phase phosphatidylcholines (Janiak et al., 1979; McIntosh, 1980; McIntosh & Simon, 1986).

The addition of cholesterol to either C24-SM or BSM bilayers disorders (or fluidizes) the hydrocarbon chains, as evidenced by the conversion of the 4.15-Å reflection to a broad wide-angle band at 4.5 Å. This disordering occurs as a consequence of cholesterol intercalating between the acyl chains and diminishing long-range chain–chain interactions. The incorporation of cholesterol into SM also adds electron density to the hydrocarbon interior of the bilayer adjacent to the polar head group (Figures 5 and 6). The most reasonable interpretation for these data is that the steroid rings of cholesterol are located in the hydrocarbon region near the lipid head group, as they are in PC bilayers (Franks, 1976; McIntosh, 1978). On the basis of the electron density profiles, cholesterol does not change the thickness of C24-SM bilayers. This observation can be rationalized in terms of cholesterol having two effects on bilayer structure, one which would tend to increase bilayer thickness and the other which would tend to decrease bilayer thickness. First, as noted for saturated phosphatidylcholines (McIntosh, 1978), the incorporation of cholesterol removes hydrocarbon chain tilt, thus tending to increase bilayer thickness. Second, cholesterol disorders the hydrocarbon chains, particularly near the center of the bilayer, tending to decrease bilayer thickness. For C24-SM bilayers, these two competing effects cancel, and the bilayer thickness is unchanged by the incorporation of cholesterol, in a similar manner as previously found for the addition of cholesterol to C(16:0)(16:0)PC bilayers (McIntosh, 1978). That the bilayer thickness of BSM is reduced by the addition of cholesterol is consistent with the idea (see above) that the hydrocarbon chain tilt is smaller in BSM bilayers than in C24-SM bilayers, so that the removal of chain tilt in BSM bilayer does not totally compensate the decrease in thickness caused by disordering of the chains.

Electron density profiles (Figures 5 and 6) show that SM/cholesterol bilayers have more pronounced terminal methyl troughs in the center of the bilayer than do SM bilayers. This implies that there is less chain interdigitation in the center of the SM/cholesterol bilayers than in SM bilayers. This may have biological significance, since many biological membranes contain both SM and lipids with symmetric hydrocarbon chains. In such membranes, high-energy voids could form in regions where SM was either located adjacent to or directly apposed to lipids with symmetric hydrocarbon chains. The presence of cholesterol would prevent the formation of such voids. We argue that this may be one reason why biological membranes containing SM also contain large concentrations of cholesterol.

*Cohesive Properties.* To determine whether the interaction of cholesterol with sphingomyelin is a consequence of hydrogen bonding between the hydroxyl group of cholesterol and the sphingosine backbone (Barenholz et al., 1980; Boggs, 1987) or is specific to the sphingomyelin acyl chains, we measured and compared the compressibility modulus of C24-SM/cholesterol bilayers to the moduli of a variety of other bilayers. Of particular interest were bilayers of equimolar cholesterol with phosphatidylcholines containing both symmetric and asymmetric acyl chain lengths. We found (Table I) that similar high values of $K$ were obtained for equimolar mixtures of cholesterol with BSM and C24-SM and with phosphatidylcholines having symmetric acyl chains [C(16:0)C(16:0)PC] and very asymmetric chains [C(22:0)C(12:0)PC and C-(12:0)C(22:0)PC]. Since cholesterol-containing bilayers made with C(16:0)C(16:0)PC, C(22:0)C(12:0)PC, and C(12:0)C-(22:0)PC all have similar values of $K$, chain asymmetry cannot be a critical factor in determining the high compressibility of SM bilayers. In particular, these data imply that cholesterol does not interact more strongly with the sphingosine chains than with a C16 hydrocarbon chain. Moreover, these data imply that the large interaction energy between sphingomyelin and cholesterol is not governed by any specific hydrogen-bond formation between the sphingosine backbone and the hydroxyl group of cholesterol, since PCs do not have the sphingosine backbone (Figure 1). Recent cholesterol exchange studies between vesicles composed of sphingomyelin derivatives have also shown that hydrogen-bond formation is not the factor giving rise to the strong cholesterol–SM interaction (Kan et al., 1991).

The data in Table I indicate that the critical factor in the interaction between cholesterol and sphingomyelin appears to be the fact that the acyl chains of SM are saturated. That is, all of the lipids tested that contained only saturated chains [C24-SM, C(16:0)C(16:0)PC, C(22:0)C(12:0)PC, and C-(12:0)C(22:0)PC] gave very high values of $K$ when incorporated into bilayers with equimolar cholesterol, whereas bilayers of 1:1 cholesterol/C(18:0)(18:1)PC and 1:1 cholesterol/C-(20:4)C(20:4)PC had significantly lower values of $K$. An interesting aspect of these results is that similar high values of $K$ are obtrained for C24-SM/cholesterol and BSM/cholesterol bilayers, even though a fraction of the BSM molecules contain unsaturated acyl chains. This result can be rationalized as follows. In BSM, the principle unsaturated fatty acid chain is nervonic acid (C24:1), which has its cis double bond between carbons 15 and 16. This means that since cholesterol is anchored to the hydrocarbon–water interface, its steroid nucleus will be in a position to interact only with the saturated region of nervonic acid. Most monosaturated fatty acids found in biological membranes, such as oleic acid [C(18:1)] have their cis double bond between carbons 9 and 10. In this position, the double bond will be in a position to interact with the cholesterol steroid nucleus in the membrane and could therefore reduce the van der Waals interaction between the steroid nucleus and the acyl chains. Similarly, arachidonic acid [C(20:4)] has cis double bonds between carbons 5 and 6, 8 and 9, 11 and 12, and 14 and 15. At least the first two of these double bonds will be positioned in the bilayer so that they can interact with the steroid nucleus. Previously, Needham and Nunn (1990) found for lipid/cholesterol bilayers that the greater the number of double bonds in the lipid acyl chain the lower the magnitude of $K$. Our data imply that the interaction of cholesterol with lipids depends

not only on the number of acyl chain double bonds but also on their position on the acyl chain. This analysis predicts that the interaction of cholesterol with SM should be similar to its interaction with lipids with saturated chains having transition temperatures similar to that of SM. To this point, Calhoun and Shipley (1979a) used differential scanning calorimetry and concluded that there is no difference in the interaction of cholesterol with C16-SM or C(14:0)C(14:0)PC.

Thus, we argue that the underlying characteristic that makes the interaction of cholesterol with sphingomyelin so strong is the ability of cholesterol to interact along its entire length with saturated acyl chains. This analysis helps to explain the high compressibility moduli of SM/cholesterol bilayers, as well as the low permeability to water and nonelectrolytes of SM/cholesterol bilayers compared to unsaturated phosphatidylcholine/cholesterol bilayers (Finkelstein, 1987).

*Summary.* In the gel phase, the acyl chains of C24-SM are tilted and partially interdigitate, so that the long C24 chain in one monolayer apposes the short sphingosine chain in the opposite monolayer. The incorporation of equimolar cholesterol removes the chain tilt and disorders the acyl chains. The compressibility modulus of C24-SM/cholesterol and BSM/cholesterol bilayers is significantly higher than that of bilayers composed of unsaturated phosphatidylcholine/cholesterol bilayers. In terms of its strong interaction with cholesterol, the critical features of the SM molecule appear to be the high degree of saturation of the hydrocarbon chains and the location of the double bond in the acyl chain.

ACKNOWLEDGMENTS

We thank Dr. Robert Bittman for many helpful discussions and for sharing with us the results of his studies prior to publication.

REFERENCES

Barenholz, Y. (1986) in *Physiology of Membrane Fluidity* (Shinitzky, M., Ed.) pp 131–173, CRC Press, Boca Raton, FL.

Barenholz, Y., & Thompson, T. E. (1980) *Biochim. Biophys. Acta 601*, 129–158.

Blaurock, A. E., & Worthington, C. R. (1966) *Biophys. J. 6*, 305–312.

Boggs, J. M. (1987) *Biochim. Biophys. Acta 906*, 353–404.

Calhoun, W. I., & Shipley, G. G. (1979a) *Biochem. Biophys. Acta 555*, 436–441.

Calhoun, W. J., & Shipley, G. G. (1979b) *Biochemistry 18*, 1717–1722.

Cohen, R., Barenholz, Y., Gatt, S., & Dagam, A. (1984) *Chem. Phys. Lipids 35*, 371–384.

Cullis, P. R., & Hope, M. J. (1980) *Biochim. Biophys. Acta 597*, 533–542.

Estep, T. N., Mountcastle, D. B., Barenholz, Y., Biltonen, R. L., & Thompson, T. E. (1979) *Biochemistry 18*, 2112–2117.

Finkelstein, A. (1987) *Water Movement through Lipid Bilayers, Pores, and Plasma Membranes. Theory and Practice*, pp 98–99, John Wiley and Sons, New York.

Franks, N. P. (1976) *J. Mol. Biol. 100*, 345–358.

Gaver, R. C., & Sweeley, C. C. (1965) *J. Am. Oil Chem. Soc. 42*, 294–298.

Herbette, L., Marquardt, J., Scarpa, A., & Blasie, J. K. (1977) *Biophys. J. 20*, 245–272.

Huang, C.-h., & Mason, J. T. (1986) *Biochim. Biophys. Acta 864*, 423–470.

Janiak, M. J., Small, D. M., & Shipley, G. G. (1976) *Biochemistry 15*, 4575–4580.

Janiak, M. J., Small, D. M., & Shipley, G. G. (1979) *J. Biol. Chem. 254*, 6068–6078.

Kan, C.-C., Ruan, Z.-s., & Bittman, R. (1991) *Biochemistry 30*, 7759–7766.

Khare, R. S., & Worthington, C. R. (1977) *Mol. Cryst. Liq. Cryst. 38*, 195–206.

Khare, R. S., & Worthington, C. R. (1978) *Biochim. Biophys. Acta 514*, 239–254.

Kwok, R., & Evans, E. (1981) *Biophys. J. 35*, 637–652.

LeNeveu, D. M., Rand, R. P., Parsegian, V. A., & Gingell, D. (1977) *Biophys. J. 18*, 209–230.

Lesslauer, W., Cain, J. E., & Blasie, J. K. (1972) *Proc. Natl. Acad. Sci. U.S.A. 69*, 1499–1503.

Levin, I. W., Thompson, T. E., Barenholtz, T. E., & Huang, C.-h. (1985) *Biochemistry 24*, 6282–6286.

Lin, H.-n., Wang, Z.-q., & Huang, C.-h. (1990) *Biochemistry 29*, 7063–7072.

Lund-Katz, S., Laboda, H. M., McLean, L. R., & Phillipis, M. C. (1988) *Biochemistry 27*, 3416–3423.

Marsh, D. (1990) *CRC Handbook of Lipid Bilayers*, p 156, CRC Press, Boca Raton, FL.

Mason, J. T., Huang, C.-h., & Biltonen, R. L. (1981) *Biochemistry 20*, 6086–6092.

Mattai, J., Stripada, P. K., & Shipley, G. G. (1987) *Biochemistry 26*, 3287–3297.

Maulik, P. R., Atkinson, D., & Shipley, G. G. (1986) *Biophys. J. 50*, 1071–1077.

McIntosh, T. J. (1978) *Biochim. Biophys. Acta 513*, 43–58.

McIntosh, T. J. (1980) *Biophys. J. 29*, 237–246.

McIntosh, T. J., & Simon, S. A. (1986a) *Biochemistry 25*, 4948–4952.

McIntosh, T. J., & Simon, S. A. (1986b) *Biochemistry 25*, 4058–4066.

McIntosh, T. J., & Holloway, P. W. (1987) *Biochemistry 26*, 1783–1788.

McIntosh, T. J., Simon, S. A., Ellington, J. C., & Porter, N. A. (1984) *Biochemistry 23*, 4038–4044.

McIntosh, T. J., Magid, A. D., & Simon, S. A. (1987) *Biochemistry 26*, 7325–7332.

McIntosh, T. J., Magid, A. D., & Simon, S. A. (1989a) *Biochemistry 28*, 17–25.

McIntosh, T. J., Magid, A. D., & Simon, S. A. (1989b) *Biophys. J. 55*, 897–904.

McIntosh, T. J., Magid, A. D., & Simon, S. A. (1989c) *Biochemistry 28*, 7904–7912.

McIntosh, T. J., Simon, S. A., Needham, D., & Huang, C.-h. (1992) *Biochemistry* (following paper in this issue).

Needham, D., & Evans, E. (1988) *Biochemistry 27*, 8261–8269.

Needham, D., & Hochmuth, R. M. (1989) *Biophys. J. 55*, 1001–1009.

Needham, D., & Nunn, R. S. (1990) *Biophys. J. 58*, 997–1009.

O'Brien, F. E. M. (1948) *J. Sci. Instrum. 25*, 73–76.

Oldfield, E., & Chapman, D. (1971) *Biochem. Biophys. Res. Commun. 43*, 610–617.

Oldfield, E., & Chapman, D. (1972) *FEBS Lett. 21*, 303–306.

Parsegian, V. A., Fuller, N., & Rand, R. P. (1979) *Proc. Natl. Acad. Sci. U.S.A. 76*, 2750–2754.

Parsegian, V. A., Rand, R. P., Fuller, N. L., & Rau, R. C. (1986) *Methods Enzymol. 127*, 400–416.

Scripada, P. K., Maulik, P. A., Hamilton, J. A., & Shipley, G. G. (1987) *J. Lipid Res. 28*, 710–718.

Serrallach, E. N., de Haas, G. H., & Shipley, G. G. (1984) *Biochemistry 23*, 713–720.

Shannon, C. E. (1949) *Proc. Inst. Radio Eng. N.Y. 37*, 10–21.

Shipley, G. G., Avecilla, L. S., & Small, D. M. (1974) *J. Lipid Res. 15*, 124-131.
Snyder, & Friere, E. (1980) *Biochim. Biophys. Acta 600*, 643-654.
Tardieu, A., Luzzati, V., & Reman, F. C. (1973) *J. Mol. Biol. 75*, 711-733.
Torbet, J., & Wilkins, M. H. F. (1976) *J. Mol. Biol. 62*, 447-458.
Vandenheuvel, F. A. (1963) *J. Am. Oil Chem. Soc. 40*, 455-463.
Vink, H. (1971) *Eur. Polym. J. 7*, 1411-1419.
Weast, R. C. (1984) *Handbook of Chemistry and Physics*, p E-42, CRC Press, Boca Raton, FL.
Wiener, M. C., Suter, R. M., & Nagle, J. F. (1989) *Biophys. J. 55*, 315-325.
Xu, H., & Huang, C.-h. (1987) *Biochemistry 26*, 1036-1043.

# Interbilayer Interactions between Sphingomyelin and Sphingomyelin/Cholesterol Bilayers†

Thomas J. McIntosh,*,‡ Sidney A. Simon,§ David Needham,∥ and Ching-hsien Huang⊥

*Departments of Cell Biology, Neurobiology, and Anesthesiology, Duke University Medical Center, Durham, North Carolina 27710, Department of Mechanical Engineering and Materials Science, Duke University, Durham, North Carolina 27706, and Department of Biochemistry, University of Virginia School of Medicine, Charlottesville, Virginia 22908*

*Received September 10, 1991; Revised Manuscript Received November 21, 1991*

ABSTRACT: Pressure versus fluid spacing relations have been obtained for sphingomyelin bilayers in the gel phase and equimolar sphingomyelin/cholesterol in the liquid-crystalline phase by the use of X-ray diffraction analysis of osmotically stressed aqueous dispersions and oriented multilayers. For interbilayer separations in the range of 5-20 Å, the repulsive hydration pressure decays exponentially with increasing fluid spacing. The decay length ($\lambda$) of this repulsive pressure is about 2 Å for both bovine brain and *N*-tetracosanoylsphingomyelin, similar to that previously found for phosphatidylcholine bilayers. However, both the magnitude of the hydration pressure and the magnitude of the dipole potential ($V$) measured for monolayers in equilibrium with liposomes are considerably smaller for sphingomyelin than for either gel or liquid-crystalline phosphatidylcholine bilayers. Addition of equimolar cholesterol increases both the magnitude of the hydration pressure and the dipole potential. These data suggest that the magnitude of the hydration pressure depends on the electric field at the interface as given by $(V/\lambda)^2$. For sphingomyelin bilayers, there is a sharp upward break in the pressure-fluid spacing relation at an interbilayer spacing of about 5 Å, indicating the onset of steric hindrance between the head groups of apposing bilayers.

The hydration pressure ($P_h$) is a short-range repulsive interaction which provides a major barrier to the close approach of apposing membranes or hydrated macromolecules (Parsegian et al., 1979; Marra & Israelachvili, 1985; Rand & Parsegian, 1989). For bilayers composed of a variety of neutral, charged, and zwitterionic lipids, the hydration pressure has been shown to decay exponentially with increasing fluid spacing ($d_f$) such that $P_h = P_o \exp(-d_f/\lambda)$, where the decay length ($\lambda$) has been measured to be 1-2 Å (LeNeveu et al., 1977; McIntosh & Simon, 1986; McIntosh et al., 1989a,c; Rand & Parsegian, 1989).

Sphingomyelin (SM) is a common membrane phospholipid that has the same phosphorylcholine head group as phosphatidylcholine (PC), but with a different backbone: SM has a sphingosine backbone and PC has a glycerol backbone. It is of interest to measure the hydration pressure between sphingomyelin bilayers for several reasons. First, although it might be expected that the hydration pressure should be similar for sphingomyelin and other phospholipid bilayers, Tamura-Lis et al. (1986) found a decay length of over 6 Å for sphingomyelin bilayers. Second, comparison of pressure–distance data from SM and PC bilayers should provide insights as to the importance of the lipid backbone in determining the hydration pressure. Third, sphingomyelin bilayers provide another test for our previously observed correlation between the magnitude of the hydration pressure ($P_o$) and the square of the dipole potential ($V$) as measured for monolayers in equilibrium with bilayers (Simon et al., 1988; McIntosh et al., 1989a–c; Simon & McIntosh, 1989). Fourth, the recent model of Israelachvili and Wennerstrom (1990) asserts that vertical displacements of the lipid head groups can give rise to a short-range repulsive pressure. This sort of steric repulsion would be expected to be significantly smaller for gel-phase bilayers than for liquid–crystalline phase bilayers, due to reduced molecular motion in the gel phase. Since SM is in the gel phase at room temperature (Calhoun & Shipley, 1979), whereas equimolar SM/cholesterol bilayers are in a liquid-crystalline phase (McIntosh et al., 1991), comparisons of pressure–distance relations between SM and equimolar SM/cholesterol bilayers should provide information on the magnitude of the proposed steric repulsion caused by vertical displacements.

In this paper, we use X-ray diffraction analysis of osmotically stressed lipid multilayers to obtain pressure–distance

† This research was supported by grants from the National Institutes of Health (GM-27278 and GM-40162).
* To whom correspondence should be addressed.
‡ Department of Cell Biology, Duke University Medical Center.
§ Departments of Neurobiology and Anesthesiology, Duke University Medical Center
∥ Department of Mechanical Engineering and Materials Science, Duke University.
⊥ Department of Biochemistry, University of Virginia School of Medicine.

0006-2960/92/0431-2020$03.00/0 